*Article*

# Formation and Texture Analysis of Extrusion-Based 3D Printed Foods Using Nixtamalized Corn and Chickpea Flours: Effect of Cooking Process

Verónica Valeria Rodríguez-Herrera [1,2] , Takumi Umeda [1] , Hiroyuki Kozu [1] and Isao Kobayashi [1,3,*]

[1] Institute of Food Research, National Agriculture and Food Research Organization, Tsukuba 305-8642, Japan; rodriguezh.veronicav18@gmail.com (V.V.R.-H.); umedat307@affrc.go.jp (T.U.); kozuh095@affrc.go.jp (H.K.)
[2] Graduate School of Science and Technology, University of Tsukuba, Tsukuba 305-8577, Japan
[3] School of Integrative and Global Majors (SIGMA), University of Tsukuba, Tsukuba 305-8577, Japan
[*] Correspondence: isaok@affrc.go.jp; Fax: +81-29-838-7997

**Featured Application: The findings of this study can inform the selection of the most appropriate post-printing process for achieving the desired final physical characteristics of 3D-printed foods.**

**Abstract:** Extrusion-based three-dimensional (3D) food printing (3DFP) enhances the customization of 3D-printed foods by using multiple food pastes. Post-printing processes like baking are usually necessary and significantly impact the stability of the 3D-printed foods. This study aimed to produce multi-material 3D-printed foods using nixtamalized corn dough and chickpea paste (CP) in extrusion-based 3DFP and to study the effect of post-printing processes (water oven cooking and steam cooking) and the type of material used (single- or multi-material) on the final appearance, weight, size, and texture of the 3D-printed foods. Multi-material 3D-printed foods were successfully produced using extrusion-based 3DFP. Steam-cooked 3D-printed foods cooked uniformly and had a better appearance, as they did not develop surface cracks compared to water oven-cooked foods. Water-oven cooked foods experienced a greater weight loss of 35.6%, and higher height and length reduction of 1.5% and 8.4%, respectively. Steam-cooked multi-material 3D-printed foods were harder at 40% of strain, with force values of 66.9 and 46.3 N for water-oven cooked foods. Post-printing processes, as well as the presence of CP in the middle of the 3D-printed foods, influenced their final appearance, weight, size, and texture. This study offers interesting findings for the innovative design of chickpea- and corn-based multi-material 3D-printed foods.

**Keywords:** 3D food printing; post-printing processes; corn-based dough; chickpea paste; texture

## 1. Introduction

Three-dimensional (3D) food printing (3DFP) represents an emerging technology in food production that is gaining popularity due to its capability to personalize food products in accordance with the nutritional requirements and preferences of individual consumers or special groups, such as older individuals [1], athletes, or kids [2]. This customization can be achieved through the creation and production of intricate foods featuring specific textures, flavors, shapes, and compositions [3,4]. Moreover, 3DFP can be considered an environmentally friendly technology, as it has the potential to reduce food waste and minimize environmental impact by utilizing low-quality fruits and vegetables [5], low-value byproducts, and low-carbon food ingredients such as algae [6], insects [7], and alternative proteins [8]. At present, four techniques are used to conduct 3DFP: extrusion-based 3DFP, selective laser sintering, binder jetting, and inkjet printing [9]. Among these methods, extrusion-based 3DFP is the most used technique [3]. In this technique, food materials are pushed through a nozzle, forming a filament. Afterwards, this filament is deposited in a pattern on the *x-y* plane, thereby forming a single layer. The process is then

repeated layer-by-layer until a 3D food product is formed [10]. The number of nozzles on a 3D food printer determines the number of food pastes that can be used alternatively to form a food product. This feature permits the simultaneous use of various food materials (e.g., different types of protein, fat, dietary fiber, vitamins, and minerals [11]) during extrusion-based 3DFP, thereby diversifying the composition, texture, shape, and taste of the 3D-printed foods and improving and benefitting their customization.

In our previous study, the printability of nixtamalized corn dough (NCD) during screw-based 3DFP was investigated [12]. NCD is a soft dough that is produced by rehydrating nixtamalized corn flour (NCF). The industrial production of NCF is based on the traditional maize preparation process from Mexico and Central America, known as "nixtamalization". In this process, maize kernels are cooked in a solution of $Ca(OH)_2$ for 1 h and steeped in cooking water with subsequent washing and grinding to produce NCD [13,14]. Currently, this process has been systemized for large-scale production, wherein the $Ca(OH)_2$ solution utilized in the traditional nixtamalization method is replaced by lye to cook the maize kernels. Afterwards, the cooked maize kernels are ground to produce a dough that is dehydrated, sifted, classified, and packaged, thereby obtaining NCF [15,16]. Then, NCF is rehydrated to obtain NCD. NCD owes its color to the type of corn from which it is made (e.g., yellow, white, blue, and red). NCD of different colors is commonly used in Mexico and other Latin American countries as raw material to produce tortillas and other corn-based products including soups, tamales, and beverages. NCD products must be cooked to make them edible. Cooking processes of NCD might include griddling, steaming, frying, or baking [12]. In our previous study, stable printability was achieved at a specific range of NCF content in the NCD, thereby permitting the obtainment of stable 3D-printed foods [12]. However, it is also necessary to study the cooking processes since they influence the stability of the printed shape [11] and the final characteristics of 3D-printed foods by modifying their texture, size, appearance, flavor, and/or composition. Vancauwenbergue et al. [17] and Horiuchi et al. [18] demonstrated that the texture of 3D-printed foods could be controlled using extrusion-based 3DFP. In addition, most of the studies focusing on the effects of cooking processes on the shape, stability, and texture of 3D-printed foods include air-frying [19], baking [20], freeze-drying [21,22], and oven-drying [22]. Nevertheless, few studies have been reported on the utilization of water oven cooking (WOC) to produce 3D-printed foods [10,23], while studies on steam cooking (SC) of 3D-printed foods have mainly focused on rice [24–26].

The objective of this study was to produce multi-material 3D-printed foods using NCD and chickpea paste (CP) in extrusion-based 3DFP and to analyze the effects of two different factors, the cooking process and type of material used, on the final characteristics of the 3D-printed foods, including appearance, weight, size, and texture. The cooking processes include WOC and SC, whereas the type of material used refers to the number of materials employed in extrusion-based 3DFP, either single- or multi-material using only NCD or NCD and CP, respectively. Foods were printed and cooked, and the weight loss, size reduction, and texture were analyzed. Chickpea (*Cicer arietinum*) was selected as the second food material due to it representing an environmentally friendly, low-cost alternative source of protein owing to its richness in essential amino acids and high digestibility [27]. Chickpea flour (CF) is also rich in minerals and micronutrients such as potassium, calcium, sodium, magnesium, copper, iron, and zinc [28]. Moreover, chickpea possesses cultural significance since it is present in traditional diets of Asian, Latin American, and African cultures in dishes such as hummus, curry, and soups [27,29]. The findings of this study can provide insights into the extent to which texture and other physical characteristics including appearance, weight, and size can be controlled by combining post-printing processes and single- or multi-material extrusion-based 3DFP.

## 2. Materials and Methods

### 2.1. Food Materials

Blue corn-based NCF containing 8.0 g/100 g protein, 4.4 g/100 g lipids, and 63.0 g/100 g carbohydrates was purchased from Sodif S.A. de C.V., Querétaro, México. Additionally, CF containing 22.3 g/100 g protein, 3.4 g/100 g lipids, and 61.2 g/100 g carbohydrates was purchased from Bob's Red Mill Natural Foods, Inc., Milwaukie, OR, USA.

### 2.2. Preparation of NCD and CP

The NCD and CP were prepared by incorporating 30 wt% NCF with 70 wt% filtered tap water for the NCD, or 55 wt% CF with 45 wt% filtered tap water for the CP. First, the required amounts of NCF and CF were weighed in a stainless-steel bowl. Afterwards, a specific volume of filtered tap water at 25 °C was poured. Subsequently, the ingredients were mixed using a cooking spatula until a uniform blend was achieved. The resulting NCD or CP was stored in a resealable plastic bag in an incubator at 25 °C until its utilization in the extrusion-based 3DFP process.

The food material-to-water weight ratios utilized in this study were determined based on previous research on the printability of NCD [12] and CP. The printability of NCD was systematically studied [12], whereas the printability of CP was investigated through a trial-and-error method based on experience acquired during previous analyses of the printability of other food materials during extrusion-based 3DFP. Stable printability was achieved for the food material/water weight ratios used in this study.

### 2.3. Extrusion-Based 3DFP

To proceed with the extrusion-based 3DFP process, two square pillars were initially designed using FreeCAD version 0.19 (Figure 1). The first square pillar corresponded to a single-material square pillar using only the NCD, with a diameter of 30 mm and a height of 10.5 mm (Figure 1a). In contrast, the second square pillar corresponded to a multi-material pillar using NCD and CP, with a diameter of 30 mm and a height of 10.5 mm (Figure 1b). The height of the second square pillar was divided into three layers: 3.0, 4.5, and 3.0 mm each. The outer 3 mm layers were formed using NCD, and the central 4.5 mm layer was formed using CP. After that, the .stl files for each of the designed square pillars were exported and uploaded to the slicer software Slic3r (version 1.2.9), where the printing parameters were established (Table 1), and the corresponding G-codes were generated. The printing parameters used (Table 1) were derived from previous research done on printability of NCD [12]. The printing speed was set to 20 mm/s. This corresponds to the speed at which the moving stage shifts. The values of the inner diameter and initial nozzle height were matched to 1.5 mm. The rate at which the 3D food printer extrudes the food paste is determined by the extrusion multiplier, which increases or decreases the screw rotation of the 3D food printer at higher or lower values, respectively. Since the printing behaviors of the NCD and CP are different, the extrusion multiplier was chosen to be 5.0 and 12.0 for the NCD and CP, respectively. This was based on previous research [12] and trials to partially march the extrusion rate and printing speed. The infill pattern was set as "Concentric", and the number of outer shells was set to two. The infill percentage was set to 100%. Subsequently, the obtained G-codes were uploaded to a graphical user interface host for 3D printing, Pronterface (version 1.6.0). Finally, a screw-based 3D food printer (FP-2500, Seiki Co., Ltd., Yonezawa, Japan) equipped with two extruders (nozzles) moved by a motor each (Figure 2a) was used to print the square pillars. Each food paste container was filled with NCD or CP until the top. After that, each square pillar, single- or multi-material, was printed ten times using the printing parameters listed in Table 1. This experiment was carried out at a constant room temperature of 25 °C, and no heating was applied in the 3D food printer.
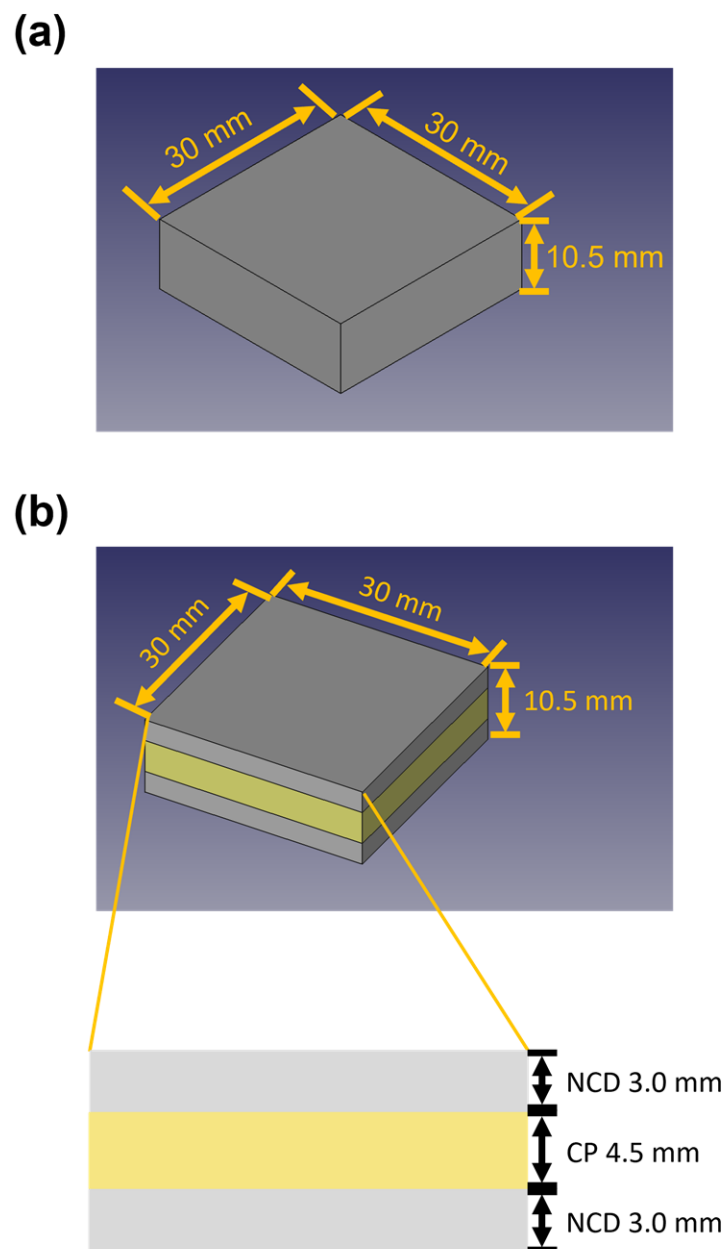
**(a)**



**(b)**



**Figure 1.** The designed three-dimensional (3D) models: (**a**) Single-material square pillar made of nixtamalized corn dough (NCD) only; (**b**) Multi-material square pillar made of NCD and chickpea paste (CP).

**Table 1.** Printing parameters.

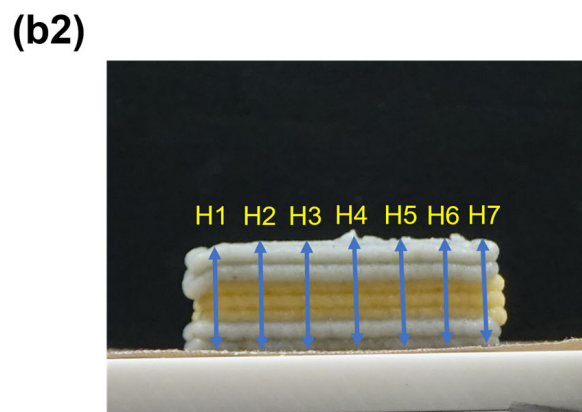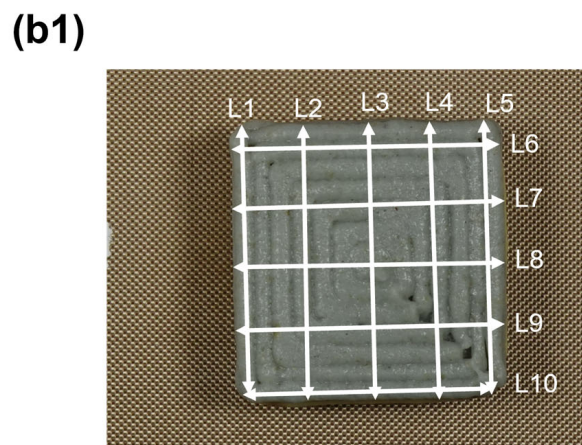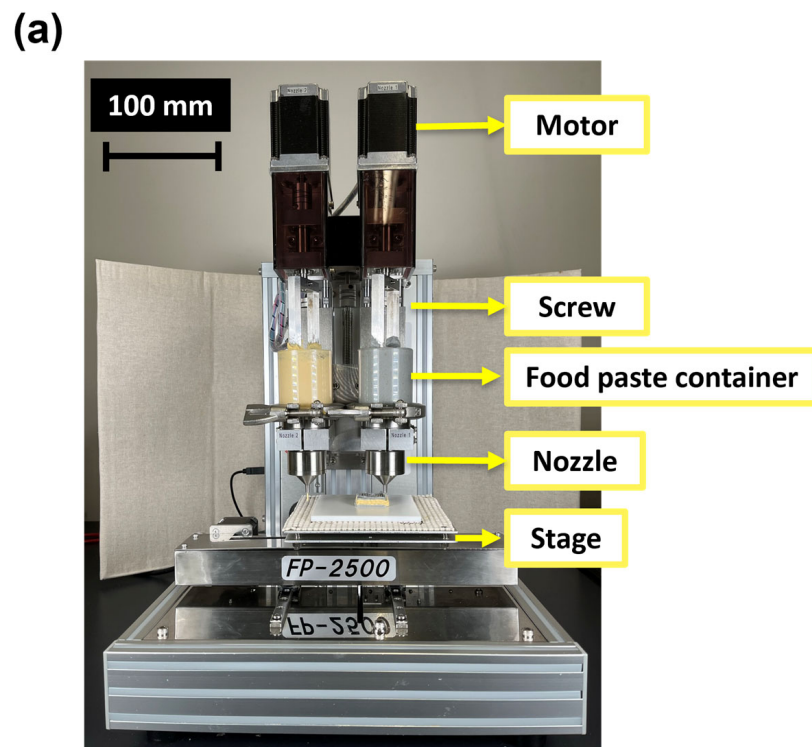| Parameter | Condition |
|---|---|
| Print speed (stage movement speed) (mm/s) | 20 |
| Nozzle inner diameter (mm) | 1.5 |
| Initial nozzle height (mm) | 1.5 |
| Extrusion multiplier for the nixtamalized corn dough (-) | 5.0 |
| Extrusion multiplier for the chickpea paste (-) | 12.0 |
| Infill pattern (-) | Concentric |
| Infill percent (%) | 100 |
| Number of outer shells (-) | 2 |
| Temperature (°C) | 25 |

**Figure 2.** (**a**) Photograph of the 3D printer used in this study; (**b**) Points of size measurements of the 3D-printed square pillars: (**b1**) Length; (**b2**) Height.

### 2.4. Post-Printing Processes of the 3D-Printed Foods

An oven (AX-XJ1; Healsio, Sharp Co., Osaka, Japan) was used to cook the 3D-printed square pillars using the WOC function. First, the oven was preheated to 100 °C. Subsequently, five of the ten 3D-printed single-material or multi-material square pillars were placed equidistantly in a tray and subjected to WOC at 100 °C for 40 min. In contrast, a steaming pot and induction cooking heater (KZ-PH33, Panasonic Holdings Co., Osaka, Japan) were used to steam the remaining five 3D-printed single-material or multi-material square pillars. First, the container of the steaming pot was filled with water until the limit was reached. The water was then heated until it reached its boiling point. Once the water was boiling, the remaining five 3D-printed single-material or multi-material square pillars were placed in the upper container of the steaming pot and steam cooked for 40 min at an approximate temperature of 98–99 °C.

After finishing the WOC or SC, the cooked 3D-printed foods were removed from the cooking devices and placed in uncovered plastic boxes for 30 min at a room temperature of approximately 25 °C. This allowed for cooling and the removal of excess heat. Afterwards, the boxes were covered with plastic lids, forming a sealed container, to gradually bring the temperature of the 3D-printed foods to room temperature approximately [10]. Finally, the cooked 3D-printed square pillars were subjected to weight, dimensional, and texture analyses.

### 2.5. Weight and Dimensional Analysis of the 3D-Printed Foods before and after Cooking

The weight and size of the raw and cooked 3D-printed square pillars were measured to assess the effects of the cooking processes, WOC or SC, and the type of material used (single- [only NCD] or multi-material [NCD + CP]).

Following the 3DFP and baking processes, the square pillars were weighted and photographed within 5 min for the raw 3D-printed foods and within 120 min for the cooked 3D-printed foods [10]. This was done once the pillars had cooled, as previously described. The images were processed using ImageJ software (version 1.53t) (National Institutes of Health, Bethesda, MD, USA) in accordance with the methodology described by Rodríguez-Herrera et al. [12] to obtain measurements of the square pillar's dimensions. The length (Figure 2(b1)) was measured at ten different points in the top view, and the average was reported as the length of the square pillar. Additionally, their heights (Figure 2(b2)) were measured at seven different points on the side view, and the average was reported as the height of the square pillar. The average and standard deviation of the weight, length, and height of the 3D-printed square pillars were calculated using five replicates for each treatment. Additionally, an acceptable range for the measured length and height was defined as ±10% of the designed size.

The weight loss percentage ($\%W_{loss}$) (Equation (1)), height reduction percentage ($\%H_{reduction}$) (Equation (2)), and length reduction percentage ($\%L_{reduction}$) (Equation (3)) were calculated and analyzed in accordance with the equations presented by Dick et al. [30], Kozu et al. [10], and Pulatsu et al. [20].

$$\%W_{loss} = \frac{W_{raw} - W_{cooked}}{W_{raw}} \times 100 \tag{1}$$

$$\%H_{reduction} = \frac{H_{raw} - H_{cooked}}{H_{raw}} \times 100 \tag{2}$$

$$\%L_{reduction} = \frac{L_{raw} - L_{cooked}}{L_{raw}} \times 100 \tag{3}$$

where $W_{raw}$ and $W_{cooked}$ represent the weights of the raw and cooked 3D-printed square pillars, respectively; $H_{raw}$ and $H_{cooked}$ are the heights of the raw and cooked 3D-printed square pillars, respectively; and $L_{raw}$ and $L_{cooked}$ indicate the lengths of the raw and cooked 3D-printed square pillars, respectively. The averages and standard deviations of these parameters were calculated from five replicates for each treatment.

### 2.6. Textural Analysis of the Cooked 3D-Printed Foods

The textural properties of the cooked 3D-printed square pillars were measured via a compression test using a texture analyzer (TA-XT plus, Stable Micro Systems Ltd., Surrey, UK) attached to a compression probe with a 75 mm diameter (P/75) at a compression strain of 80% [10]. The test parameters used were as follows: pre-test and test speed of 1 mm/s, post-test speed of 10 mm/s, and trigger force of 0.049 N. All the experiments were conducted at a room temperature of 25 °C. Five replicates of each treatment were used to obtain the strain-force curves of the cooked square pillars. Furthermore, the forces required to reach 40% and 80% of the strain were obtained from the strain-force curves. The averages and standard deviations were calculated using five replicates for each treatment.

### 2.7. Statistical Analysis

To assess the effect of the cooking process and the type of material utilized on the characteristics of the 3D-printed square pillars, a completely randomized design with a $2 \times 2$ factorial treatment structure was employed. The variation factors were Factor 1 (F1), which corresponded to the type of material used, including single-material (NCD) and multi-material (NCP + CP), and Factor 2 (F2), which corresponded to the cooking process, including WOC and SC. This resulted in four different treatments: (1) NCD-WOC, (2) NCD-SC, (3) NCD + CP-WOC, and (4) NCD + CP-SC. The responses of five replicates of $\%W_{loss}$, $\%H_{reduction}$, $\%L_{reduction}$, force at 40% strain, and force at 80% strain were subjected to analysis of variance and means comparison routines using the Tukey test, with a significance level of 0.05 (Table 2). Statistical software Minitab® version 21.4.2 was utilized.

**Table 2.** Mean differences for weight loss percentage, height reduction percentage, length reduction percentage, force at 40% strain, and force at 80% strain in factor 1: Type of material used, factor 2: Cooking process, and the combination of factors 1 and 2.

| Factor/Variable | | Weight Loss Percentage (%) | Height Reduction Percentage (%) | Length Reduction Percentage (%) | Force at 40% Strain (N) | Force at 80% Strain (N) |
|---|---|---|---|---|---|---|
| F1: Material * | NCD | 17.07 ± 18.68 A | 10.69 ± 6.89 A | 0.90 ± 6.75 A | 28.61 ± 6.56 B | 154.27 ± 13.81 B |
| | NCD + CP | 13.97 ± 17.29 B | 8.87 ± 1.37 A | 2.48 ± 2.90 A | 84.64 ± 33.79 A | 246.62 ± 29.11 A |
| F2: Cooking process * | WOC | 33.33 ± 2.56 A | 7.10 ± 3.15 B | 5.88 ± 1.95 A | 46.32 ± 22.70 B | 193.77 ± 41.75 A |
| | SC | −2.29 ± 3.39 B | 12.46 ± 5.17 A | −2.50 ± 4.03 B | 66.92 ± 45.02 A | 207.12 ± 58.92 A |
| F1 & F2: Material & Cooking process ** | NCD-WOC | 35.53 ± 1.67 A | 4.56 ± 2.38 C | 7.06 ± 2.12 A | 29.64 ± 6.22 B | 158.39 ± 16.42 B |
| | NCD-SC | −1.39 ± 3.64 B | 16.81 ± 3.79 A | −5.26 ± 3.27 C | 27.57 ± 6.73 B | 150.14 ± 8.82 B |
| | NCD + CP-WOC | 31.13 ± 0.81 A | 9.64 ± 1.14 B | 4.70 ± 0.57 AB | 63.01 ± 20.87 B | 229.15 ± 26.70 A |
| | NCD + CP-SC | −3.19 ± 2.84 B | 8.11 ± 1.12 BC | 0.26 ± 2.57 B | 106.26 ± 30.21 A | 264.10 ± 19.27 A |

NCD Nixtamalized Corn Dough. CP Chickpea paste. WOC Water oven cooking. SC Steam cooking. F1: Material Factor 1: Type of material used. F2: Cooking process Factor 2: Cooking process. F1 & F2: Material & Cooking process Combination of factor 1 and factor 2. * Each value is expressed as mean ± SD of 10 replicates for F1 and F2, while for F1 & F2, the number of replicates is 5. ** Different alphabets in the same column of each factor indicate that the data are significantly different with $p < 0.05$ by Tukey's test.

## 3. Results and Discussion

### 3.1. Appearance

Successful extrusion-based 3DFP was achieved in the four treatments: (1) NCD-WOC, (2) NCD-SC, (3) NCD + CP-WOC, and (4) NCD + CP-SC (Figure 3). After WOC, cracks on the surface of the 3D-printed square pillars were visible in both the NCD-WOC and NCD + CP-WOC treatments. Cracks on the surface of 3D-printed foods made of rice starch and cookie dough prepared with tapioca flour, shortening, and non-fat milk were also observed after roasting and microwaving [24], and baking [20], respectively. This was attributed to the increased void gaps and moisture loss during roasting and microwaving [24]. In contrast, no formation of cracks was observed on the surface of the steam-cooked 3D-printed square pillars (NCD-SC and NCDP + CP-SC treatments). Similar results were obtained after steaming 3D-printed foods made of rice starch [24], rice flour [25], and a mix

of rice flour, jaggery, and water [26], where steaming did not cause the formation of cracks on the surface of the 3D-printed foods. The formation of cracks on the surface of the water oven-cooked 3D-printed square pillars may be attributed to the loss of water during the WOC process, whereas during the SC process, the steam surrounding the 3D-printed square pillars does not allow the loss of water, avoiding the formation of cracks on the surface of the food. These results showed that the appearance of the steam-cooked 3D-printed square pillars was better than that of the water oven-cooked pillars.
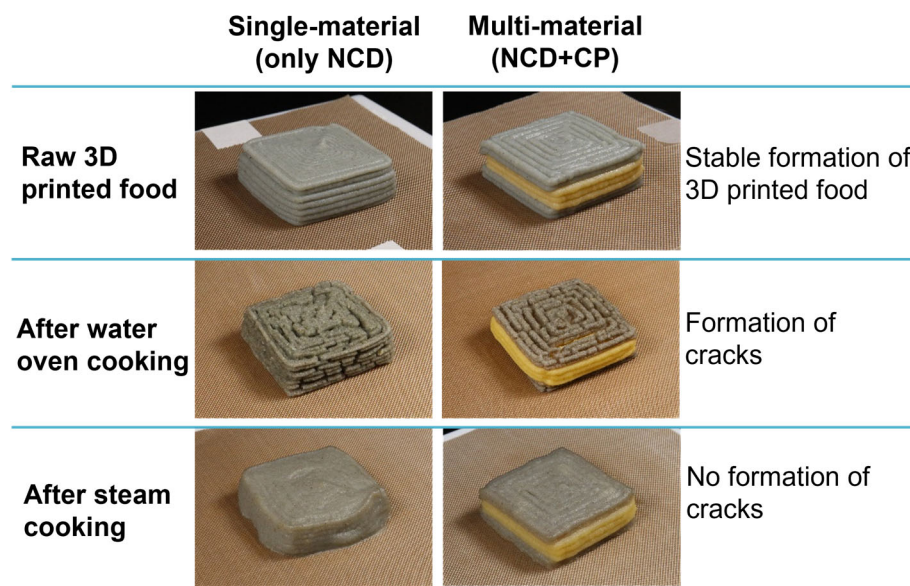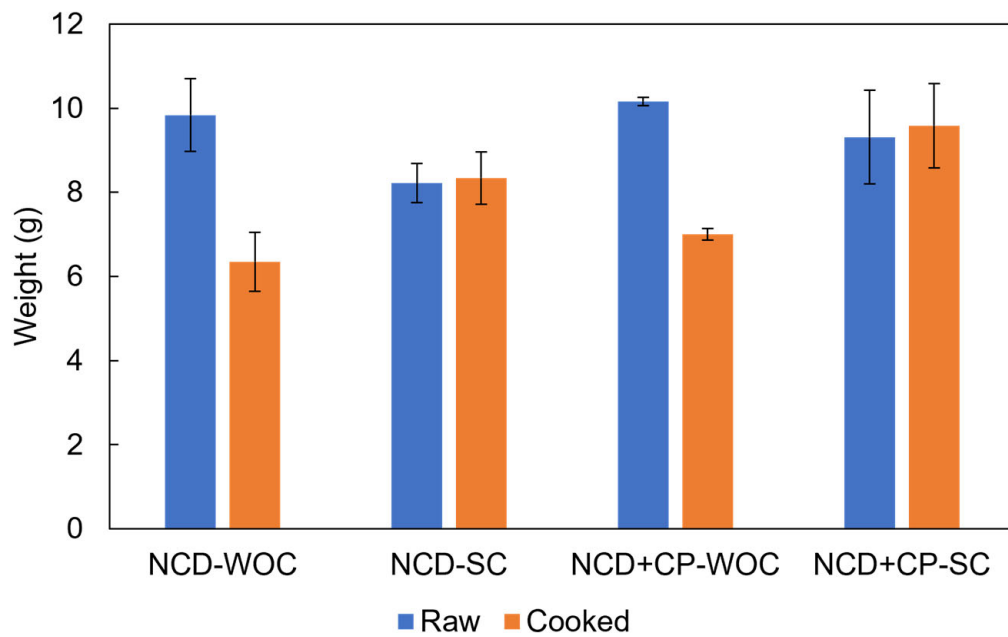


**Figure 3.** Photographs of the raw and cooked 3D-printed square pillars (NCD: Nixtamalized corn dough, CP: Chickpea paste).

*3.2. Weight*

The weights of the raw 3D-printed square pillars were 9.83 g, 8.22 g, 10.16 g, and 9.31 g in NCD-WOC, NCD-SC, NCD + CP-WOC, and NCD + CP-SC, respectively (Figure 4(a1)). However, after WOC, the weight decreased to 6.35 g in NCD-WOC and 7.00 g in NCD + CP-WOC, while after SC, the weight increased to 8.34 g in NCD-SC and 9.58 g in NCD + CP-SC. In addition, Figure 4(a2) shows that WOC caused a weight decrease of 35.53% and 31.13% in NCD-WOC and NCD + CP-WOC, respectively. In contrast, the negative values of %$W_{loss}$ in NCD-SS and NCD + CP-SC showed that the weight of the steam-cooked square pillars did not decrease but increased after SC, with %$W_{loss}$ values of −1.39% and −3.19%, respectively. Additionally, extensive differences between the means of F1 (type of material used) and F2 (cooking process) in Table 2 show that both factors affected the %$W_{loss}$. Regarding F1, a higher %$W_{loss}$ in NCD was observed in comparison with the %$W_{loss}$ of NCD + CP treatments. This behavior might have occurred due to higher water content in NCD which caused a greater water loss during cooking processes, resulting in a higher %$W_{loss}$ in comparison to NCD + CP treatments, where the water content was smaller, resulting in less water loss and %$W_{loss}$. As for F2, the weight decrease of the water oven-cooked square pillars may have been due to the loss of water during the cooking process. In contrast, the weight increase during the SC process may have been due to the addition of moisture during SC [26]. A study observed a greater weight decrease in rice starch 3D-printed foods after dry-heat cooking processes, including roasting and microwaving, in comparison with steaming [24]. This was attributed to the increased void gaps and moisture loss during roasting and microwaving [24]. However, one main difference between the results reported by Theagarajan et al. [24] and the results of this study is that rice starch 3D-printed foods also exhibited a weight decrease after steaming, whereas the weight of 3D-printed foods made of NCD and CP increased after SC. Additionally, a weight increase after steaming 3D-printed foods made of jaggery was also reported by Thangalakshmi

et al. [26]. The reason for these different behaviors of $\%W_{loss}$ after SC might be attributed to the different steaming times. Rice starch 3D-printed foods [24] were steamed for two min, whereas in this study and the one presented by Thangalakshmi et al. [26], steaming times of 40 and 15 min, respectively, were used. Moreover, Dong et al. [31], reported that $\%W_{loss}$ is influenced by the water-holding capacity of the materials. Therefore, studying the water-holding capacity of the food materials used could provide a more comprehensive understanding of the food material's behavior during different cooking processes.
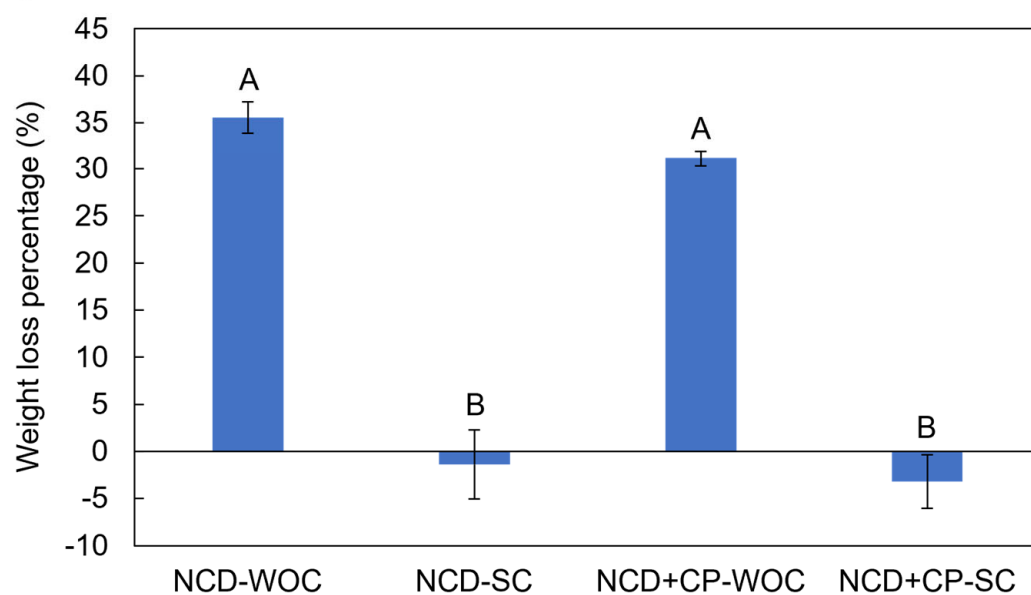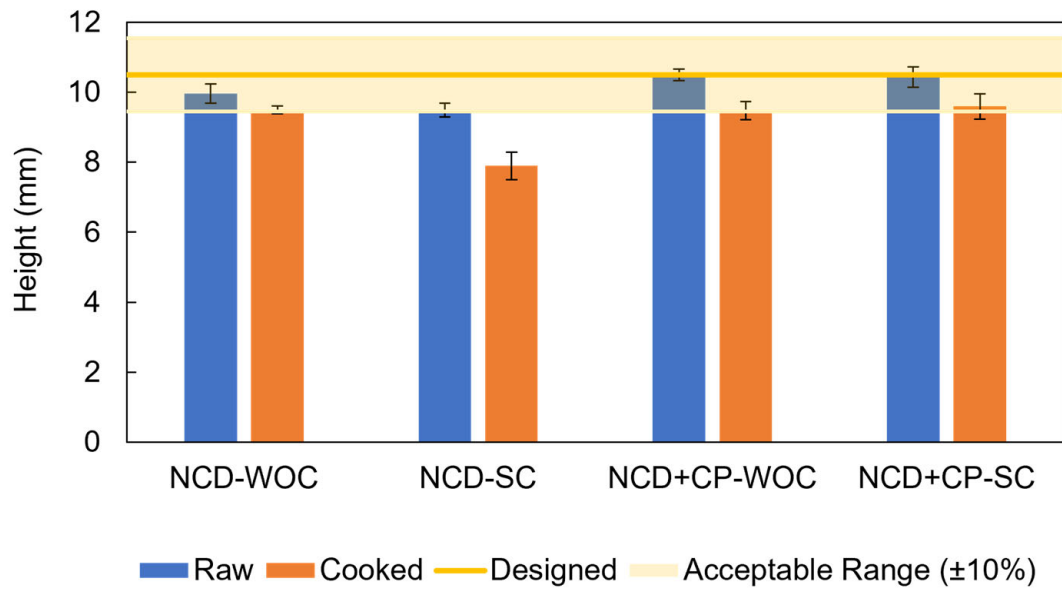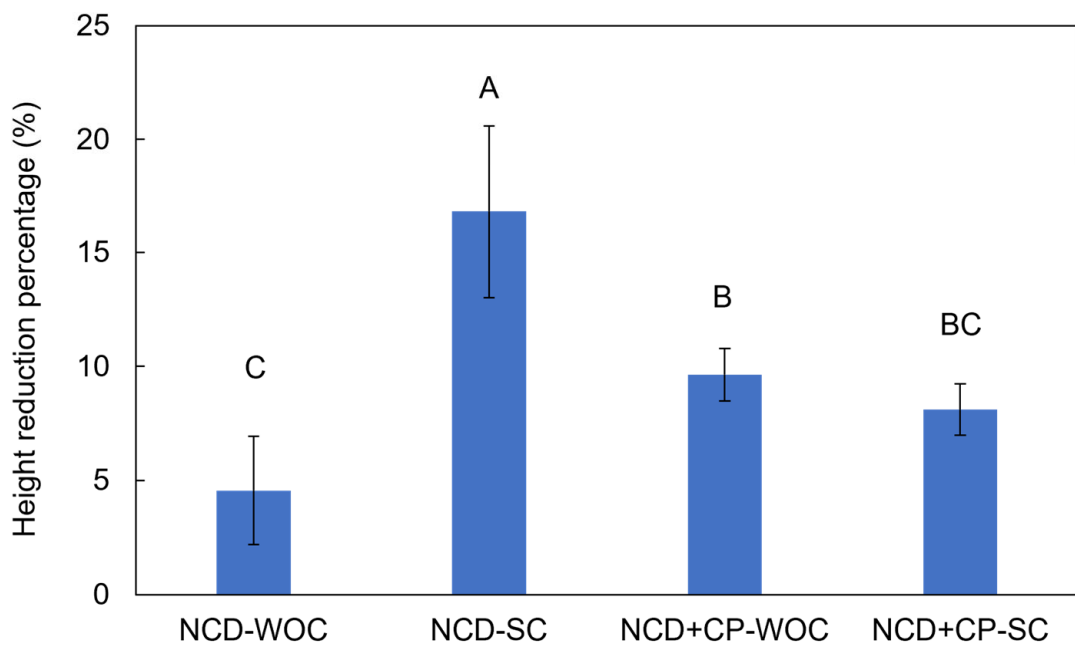
**(a1)**



**(a2)**



**Figure 4.** *Cont.*

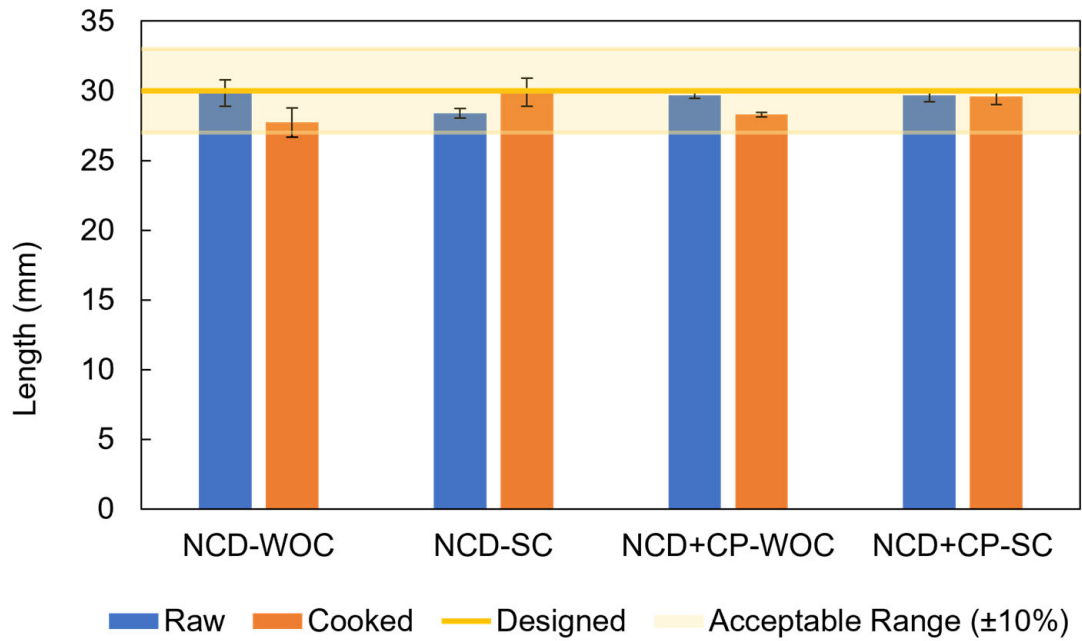**(b1)**



**(b2)**



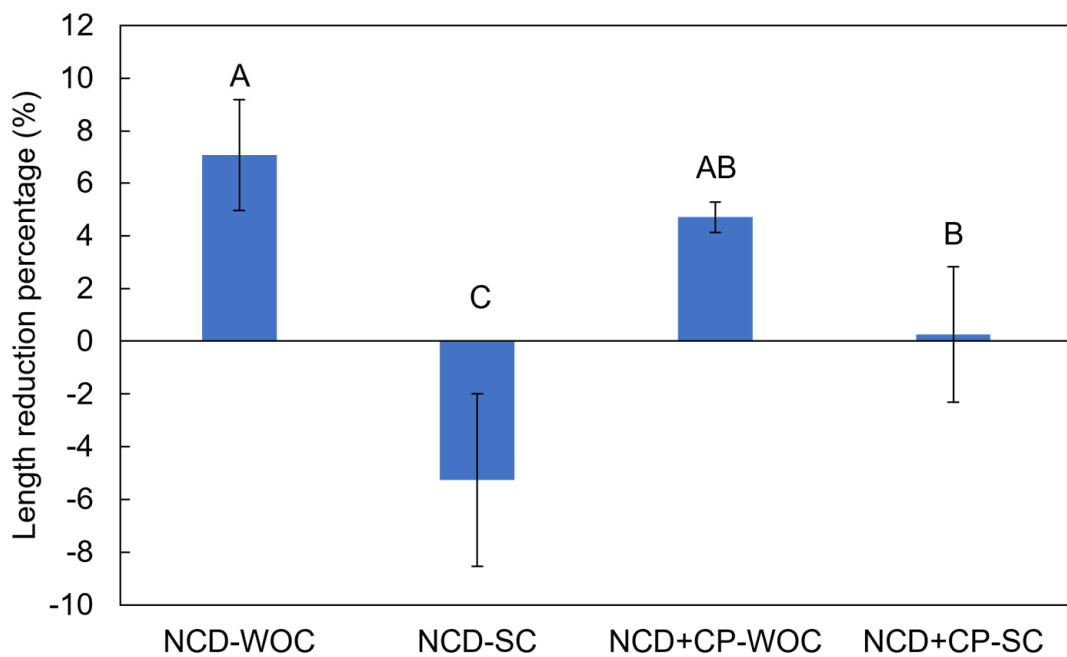**Figure 4.** *Cont.*

**(c1)**



**(c2)**



**Figure 4.** (**a1**) Weight of the raw and cooked 3D-printed square pillars; (**a2**) Weight loss percentage after cooking; (**b1**) Height of the raw and cooked 3D-printed square pillars; (**b2**) Height reduction percentage after cooking; (**c1**) Length of the raw and cooked 3D-printed square pillars; (**c2**) Length reduction percentage after cooking (NCD: Nixtamalized corn dough, CP: Chickpea paste, WOC: Water oven cooking, SC: Steam cooking) (plots and error bars represent the mean and standard deviation of five repeated measurements for each treatment) (Different alphabets in the bars indicate that the data are significantly different with $p < 0.05$ by Tukey's test).

### 3.3. Size

In Figure 4(b1,c1), the heights and lengths of the raw 3D-printed square pillars are very close to those of the designed 3D models for the four treatments. These values are within the acceptable range established as $\pm 10\%$ of the designed dimensions. These results confirm the successful single- and multi-material extrusion-based 3DFP process.

Figure 4(b2,c2) show the $\%H_{reduction}$ and $\%L_{reduction}$ of the four treatments, respectively. After WOC, the heights ($\%H_{reduction}$) of the NCD-WOC and NCD + CP-WOC decreased by 4.56% and 9.64%, respectively, with respect to the height of the raw 3D-printed square pillar. Additionally, the height of the steam-cooked square pillars was reduced by 16.81% and 8.11% for NCD-SC and NCD + CP-SC, respectively. Regarding the length ($\%L_{reduction}$) of the 3D-printed square pillars, major reductions of 7.06% and 4.70% in the NCD-WOC and NCD + CP-WOC treatments, respectively, were observed for the square pillars subjected to WOC. In contrast, the length of the square pillars subjected to SC only decreased by 0.26% in the NCD + CP-SC treatment and even increased by $-5.26\%$ in the NCD-SC treatment. This study hypothesized that WOC would lead to a higher $\%H_{reduction}$ and $\%L_{reduction}$ owing to a higher loss of water in comparison with SC, where slighter $\%H_{reduction}$ and $\%L_{reduction}$ were expected. This behavior could be observed in multi-material treatments including NCD + CP-WOC and NCD + CP-SC, where the larger loss of water in the square pillars of NCD + CP-WOC might have led to a larger $\%H_{reduction}$ and $\%L_{reduction}$ in comparison with the square pillars of NCD + CP-SC, where the loss of water was lower. However, NCD-SC treatment did not present the same behavior since a large $\%H_{reduction}$ and a negative value of $\%L_{reduction}$ indicating an increase of length were presented. This specific behavior of NCD-SC treatment may be due to localized condensation during SC, leading to wetting and the eventual weakening and collapse of the structure.

Regarding the influence of F1 and F2 on the means of $\%H_{reduction}$ and $\%L_{reduction}$, Table 2 shows that no significant difference was found between the means of $\%H_{reduction}$ and $\%L_{reduction}$ in F1. This means that $\%H_{reduction}$ and $\%L_{reduction}$ were not influenced by the type of material used, that is, either NCD or NCD + CP. In contrast, a marked difference was found between the means of $\%H_{reduction}$ and $\%L_{reduction}$ in F2, indicating that the type of cooking process influenced the $\%H_{reduction}$ and $\%L_{reduction}$ of the 3D-printed foods. For instance, in Table 2, the $\%H_{reduction}$ in F2 was higher in SC (12.46%) than in WOC (7.10%), while the $\%L_{reduction}$ in F2 was higher in WOC (5.88%) than in SC ($-2.50\%$) where the negative value of $\%L_{reduction}$ in SC indicates that the length of the square increased after SC.

A previous study observed that the shape fidelity and shrinkage of rice starch 3D-printed foods were higher after steaming than after dry-heat cooking processes, such as roasting or microwaving [24]. These findings are similar to those presented in NCD + CP-WOC and NCD + CP-SC, where a slightly lower $\%H_{reduction}$ and $\%L_{reduction}$ were obtained for NCD + CP-SC than for NCD + CP-WOC (Figure 4(b1,b2,c1,c2)). These behaviors may be attributed to the cooking medium, as moist-heat cooking processes like steaming may enhance moisture retention [24]. Furthermore, Liu et al. [25] conducted studies on steamed rice dough-based 3D printed foods and emphasized the effect of swelling capacity on shape fidelity, where amylose and amylopectin contents of the rice can influence the swelling capacity of the 3D-printed foods during steaming and, eventually, on the shape fidelity. Swelling of the starch of the NCD during SC due to water absorption may have contributed to the results presented in this study, wherein better shape fidelity was observed after SC rather than after WOC. However, a more detailed analysis of the compositions and morphological structures of the food materials is needed and would help clarify this hypothesis.

### 3.4. Texture

The strain-force curves of the cooked 3D-printed square pillars are shown in Figure 5a. In general, the strain-force curves had an S-shape. This type of behavior is common in breads, cakes, other highly aerated deformable foods, and some cheeses [32]. However,

the strain-force curves of NCD + CP-WOC and NCD + CP-SC showed a large S-shape in comparison to the strain-force curves of NCD-WOC and NCD-SC which showed a slight S-shape. This behavior may be due to the presence of a CP phase with different hardness values in the intermediate phase of the 3D-printed square pillars. Three different regions are identified in the S-shaped curve: (1) linear elastic, (2) plastic buckling, and (3) densification [33]. The linear elastic region is at the beginning of the curve. If a sample is loaded only within this region, no permanent deformation occurs. The linear elastic region of the cooked 3D-printed square pillars exhibited a J-shape. This indicated that the stress increased at a faster rate than the strain as energy was added to the samples. This permits the 3D-printed square pillars to withstand higher levels of stress before reaching the yield stress, which is the stress where a material transitions from the elastic to the plastic region [34]. The slope of the linear elastic region was found to be 0.83 for NCD-SC, 1.22 for NCD-WOC, 2.27 for NCD + CP-WOC, and 3.91 for NCD + CP-SC. This suggests that multi-material treatments including NCD + CP-WOC and NCD + CP-SC exhibited greater resistance than single-material treatments, NCD-WOC and NCD-SC. This is evidenced by the necessity for a higher force to achieve the same strain. The plastic buckling region is characterized by a plateau region, which is associated with the collapse of the cells. In this region, permanent deformation occurs [34,35]. The plastic buckling region of the cooked 3D-printed square pillars of NCD-WOC and NCD-SC is relatively small, indicating that they are unable to absorb a significant amount of energy. In contrast, the plastic buckling region of NCD + CP-WOC and NCD + CP-SC is larger. These results suggest that the incorporation of CP into the multi-material square pillars enables them to absorb a greater amount of energy in comparison with single-material square pillars. Finally, in the densification region, the stress increases at a higher rate due to the occurrence of microscopic changes in the material as it plastically deforms, thereby enhancing its strength and reflecting material densification [34,36]. Following this point, the samples may attain the ultimate compressive strength, which represents the maximum stress experienced by the material prior to fracture.
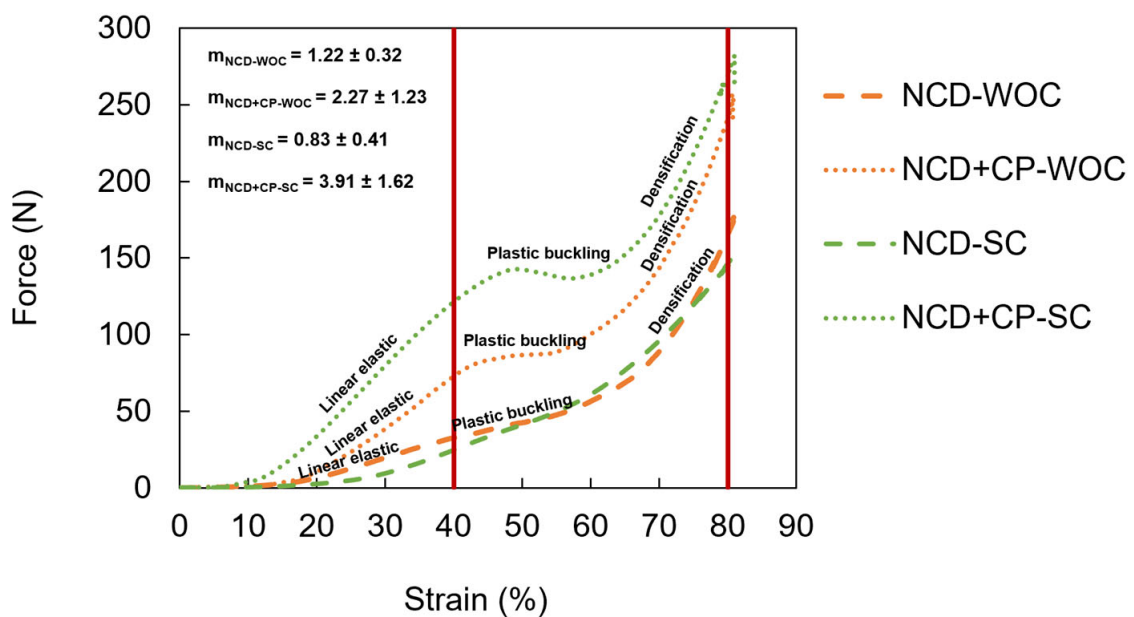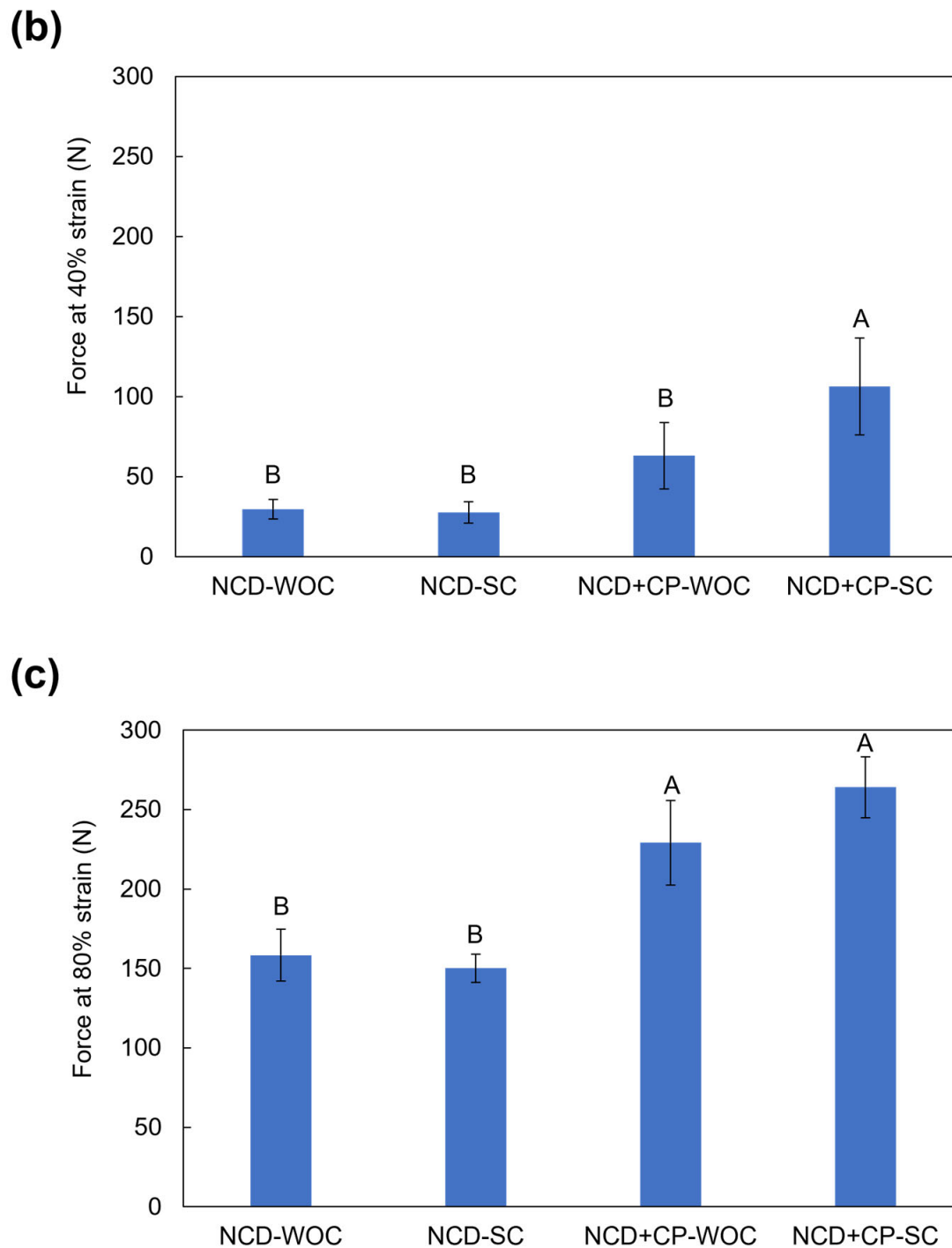
**(a)**



**Figure 5.** *Cont.*

**(b)**



**(c)**



**Figure 5.** Texture of the cooked 3D-printed square pillars: (**a**) Strain-force curves (**b**) Force at 40% of strain; (**c**) Force at 80% of strain. (NCD: Nixtamalized corn dough, CP: Chickpea paste, WOC: Water oven cooking, SC: Steam cooking, m: slope of the linear elastic region) (Plots and error bars represent the mean and standard deviation of five repeated measurements) (Different alphabets in the bars indicate that the data are significantly different with $p < 0.05$ by Tukey's test).

In Figure 5b,c, the forces required to reach 40 and 80% of the strain, are shown, respectively. Force at 40% and 80% of strain were selected for analysis since the former is within the linear elastic region, prior to reaching the plastic buckling region. This may provide insights into the initial deformation of the 3D-printed square pillars. Moreover, it is close to the failure point which reflects the internal structure failure of the 3D-printed foods.

In contrast, force at 80% of strain falls within the upper detection limit of the load cell of the texture analyzer [10]. The forces needed to reach 40% of strain in NCD-WOC and NCD-SC were 29.64 and 27.57 N, respectively. On the contrary, for the multi-material treatments, NCD + CP-WOC and NCD + CP-SC, the forces needed to reach 40% strain were 63.01 and 106.26 N, respectively. The same behavior was observed in the force needed to reach 80% strain, where in the single material treatments, NCD-WOC and NCD-SC, the values were 158.39 and 150.14 N, respectively, while for the multi-material treatments, NCD + CP-WOC and NCD + CP-SC, the values were 229.15 and 264.10 N, respectively. The following two key findings are presented in Table 2. First, factor F1 influenced both variables, force at 40% strain and force at 80% strain, where the multi-material foods (NCD + CP) were harder than the single-material foods (NCD). The presence of CP in the intermediate phase of the 3D-printed square pillars might have influenced these results because the carbohydrates and proteins of the CP might have formed special structures after cooking as a result of heat addition, such as protein gelation and starch gelatinization. Second, factor F2 influenced the force at 40% strain, where the steam-cooked 3D-printed square pillars were harder than the water oven-cooked ones. The presence of water in the steam-cooked 3D-printed square pillars may have led to a higher slope of the linear elastic region compared to the water oven-cooked 3D-printed square pillars, where the water inside their structure was replaced by air, which led to a lower linear elastic region. In contrast, factor F2 did not influence the force at 80% strain, and no significant difference was found between the hardness of the steam-cooked and water oven-cooked 3D-printed square pillars. This behavior might be due to the slope of the densification region of the strain-force curves of the water oven-cooked 3D-printed square pillars being higher than that of the steam-cooked pillars. Water oven-cooked 3D-printed square pillars might be prone to higher densification than steam-cooked pillars because of the absence of water.

An earlier study reported that steamed rice starch 3D-printed foods exhibited a softer texture than roasted or microwaved foods [24], a finding that contrasts with the results of the present study, in which steam-cooked 3D-printed foods demonstrated a harder texture than water oven-cooked foods within the linear elastic region. Given the inherent complexity in comparing studies due to the differences in food materials and their compositions, cooking processes and their cooking times, as well as the methods of texture analysis applied, it becomes challenging to ascertain the underlying cause of this observed difference.

### 3.5. General Discussion and Future Prospects

In general, during WOC, the loss of water resulted in a greater decrease in the weight and shrinkage of the 3D-printed square pillars. Furthermore, it induced the formation of cracks on the surface. In contrast, during SC, lower water loss resulted in less shrinkage and a smaller decrease in weight. In addition, the steam-cooked 3D-printed square pillars had a better appearance, because cracks were not formed on the surface. Similar results were found by Theagarajan et al. [24], where the formation of cracks and higher shrinkage were observed in microwaved square pillars made of rice starch compared to steamed ones. Kozu et al. [10] also reported shrinkage of 3D-printed foods after WOC. Because the temperature of gelatinization of starch shifts to higher temperatures under conditions of limited water availability [37], the temperature of gelatinization of the starch contained in the water oven-cooked square pillars might have increased, leading to lower gelatinization and weaker structure formation in comparison with the very well-gelatinized steam-cooked square pillars. This behavior might also have led to more homogenous steam-cooked square pillars than water oven-cooked ones. However, the steam-cooked multi-material square pillars were harder than the water oven-cooked multi-material square pillars. The steam-cooked 3D-printed square pillars made of rice starch were softer than the microwaved ones [24]. The presence of CP in the middle of the 3D-printed square pillars may have influenced this result. Overall, the SC process may be more convenient because the appearance, size, and weight of the 3D-printed square pillars were not significantly affected.

In the future, analysis of the microstructure of the cooked 3D-printed square pillars through microscopic techniques, including scanning electron microscopy, may help elucidate the effects of cooking processes and food composition on the surface morphology of the 3D-printed foods. Furthermore, it is important to investigate the impact of cooking processes and food materials on the nutritional properties of 3D-printed foods. This can be achieved through proximate analysis, digestibility studies, and the identification of noteworthy nutrients, including proteins, to understand their interaction with consumers. Additionally, as this study only evaluated a single condition of time and temperature during the cooking process, a more comprehensive analysis employing different temperatures and cooking times could determine optimal conditions for WOC and SC. Moreover, sensory evaluation, with a particular emphasis on the texture and appearance of 3D-printed foods, can offer insights into consumer preferences and acceptability. Finally, the inclusion of other cooking processes, such as frying or baking could provide valuable insights into the changes undergone by 3D-printed foods during the cooking processes.

## 4. Conclusions

In this study, multi-material 3D-printed foods using NCD and CP were successfully produced using extrusion-based 3DFP with two nozzles. The results showed that $\%H_{reduction}$ and $\%L_{reduction}$ were not affected by the type of material used in the 3D-printed square pillars (NCD or NCD + CP). Nevertheless, the $\%W_{loss}$, force at 40% strain, and force at 80% strain were affected by the type of material used, where 3D-printed square pillars made of NCD + CP produced less $\%W_{loss}$ and a higher force at 40% strain and 80% strain in comparison with the 3D-printed square pillars made only using NCD. Less $\%W_{loss}$ in the 3D-printed square pillars made of NCD + CP might have occurred because of the lower water content compared to the 3D-printed square pillars made of only NCD. Furthermore, the presence of CP, with different hardness values due to protein gelation and starch gelatinization in the mid-section of the multi-material 3D-printed foods, might have led to a higher force at 40% and 80% strain. Regarding cooking processes, higher water loss during WOC resulted in higher $\%W_{loss}$ and $\%L_{reduction}$ in comparison to SC. In contrast, SC produced harder 3D-printed square pillars at 40% strain owing to the presence of water in the steam-cooked 3D-printed square pillars compared to the water oven-cooked pillars, where the water inside their structure is replaced by air. However, the force at 80% strain was not affected by the cooking process because the water oven-cooked 3D-printed square pillars might be prone to higher densification owing to the absence of water in comparison to the steam-cooked ones. In general, SC was found to be the most suitable cooking process because the appearance, size, and shape of the 3D-printed foods were not significantly affected.

From an application and technology viewpoint, the findings obtained in this study suggest the possibility of producing 3D-printed foods using two food materials, NCD and CP, and improving their appearance and texture, as well as maintaining their 3D-shape stability through cooking processes including WOC and SC. These findings are expected to be useful for the innovative design of chickpea- and corn-based multi-material 3D-printed foods.

## References

1. Xie, Y.; Liu, Q.; Zhang, W.; Yang, F.; Zhao, K.; Dong, X.; Prakash, S.; Yuan, Y. Advances in the Potential Application of 3D Food Printing to Enhance Elderly Nutritional Dietary Intake. *Foods* **2023**, *12*, 1842. [CrossRef]
2. Derossi, A.; Caporizzi, R.; Azzollini, D.; Severini, C. Application of 3D printing for customized food. A case on the development of a fruit-based snack for children. *J. Food Eng.* **2018**, *220*, 65–75. [CrossRef]
3. Gholamipour-Shirazi, A.; Kamlow, M.; Norton, I.T.; Mills, T. How to Formulate for Structure and Texture via Medium of Additive Manufacturing—A Review. *Foods* **2020**, *9*, 497. [CrossRef]
4. Pereira, T.; Barroso, S.; Gil, M.M. Food Texture Design by 3D Printing: A Review. *Foods* **2021**, *10*, 320. [CrossRef]
5. Pant, A.; Ni Leam, P.X.; Chua, C.K.; Tan, U. Valorisation of vegetable food waste utilising three-dimensional food printing. *Virtual Phys. Prototyp.* **2023**, *18*, e2146593. [CrossRef]
6. Thakur, R.; Yadav, B.K.; Goyal, N. An Insight into Recent Advancement in Plant- and Algae-Based Functional Ingredients in 3D Food Printing Ink Formulations. *Food Bioprocess. Technol.* **2023**, *16*, 1919–1942. [CrossRef]
7. Soares, S.; Forkes, A. Insects au gratin -an investigation into the experiences of developing a 3d printer that uses insect protein based flour as a building medium for the production of sustainable food. In *E&PDE14, DS78: Proceedings of the 16th International Conference on Engineering and Product Design Education, University of Twente, Enschede, The Netherlands, 4–5 September2014 "Design Education & Human Technology Relations"*; Bohemia, E., Eger, A., Eggink, W., Kovacevic, A., Parkinson, B., Wits, W., Eds.; The Design Society: Glasgow, UK; Institution of Engineering Designers: Wiltshire, UK, 2014.
8. Chen, Y.; Zhang, M.; Phuhongsung, P. 3D printing of protein-based composite fruit and vegetable gel system. *LWT* **2021**, *141*, 110978. [CrossRef]
9. Liu, Z.; Zhang, M. 3D Food Printing Technologies and Factors Affecting Printing Precision. In *Fundamentals of 3D Food Printing and Applications*; Godoi, F.C., Bhandari, B.R., Prakash, S., Zhang, M., Eds.; Academic Press: Cambridge, MA, USA, 2019; pp. 19–40, ISBN 9780-1281-4564-7.
10. Kozu, H.; Umeda, T.; Kobayashi, I. Production and characterization of 3D-printed foods with hybrid layered structures consisting of agricultural product-derived inks. *J. Food Eng.* **2024**, *360*, 111720. [CrossRef]
11. Demei, K.; Zhang, M.; Phuhongsung, P.; Mujumdar, A.S. 3D food printing: Controlling characteristics and improving technological effect during food processing. *Food Res. Int.* **2022**, *156*, 111120. [CrossRef]
12. Rodríguez-Herrera, V.V.; Umeda, T.; Kozu, H.; Sasaki, T.; Kobayashi, I. Printability of Nixtamalized Corn Dough during Screw-Based Three-Dimensional Food Printing. *Foods* **2024**, *13*, 293. [CrossRef]
13. International Maize and Wheat Improvement Center. Available online: https://www.cimmyt.org/news/what-is-nixtamalization/ (accessed on 6 November 2022).
14. Arendt, E.K.; Zannini, E. Maizes. In *Cereal Grains for the Food and Beverage Industries*; Woodhead Publishing: Sawston, UK, 2013; pp. 67–115, ISBN 9780-8570-9413-1.
15. Flores-Farías, R.; Martínez-Bustos, F.; Salinas-Moreno, Y.; Ríos, E. Caracterización de harinas comerciales de maíz nixtamalizado. *Agrociencia* **2002**, *36*, 557–567.
16. Rooney, L.W.; Suhendro, E.L. Perspectives on nixtamalization (alkaline cooking) of maize for tortillas and snacks. *Cereal Foods World* **1999**, *44*, 466–470.
17. Vancauwenberghe, V.; Delele, M.A.; Vanbiervliet, J.; Aregawi, W.; Verboven, P.; Lammertyn, J.; Nicolaï, B. Model-based design and validation of food texture of 3D printed pectin-based food simulants. *J. Food Eng.* **2018**, *231*, 72–82. [CrossRef]
18. Horiuchi, M.; Akachi, T.; Kawakami, M.; Furukawa, H. Texture Design and Its Effect of Soft Foods Suitable for Nursing Foods Using Macroscopic 3D Structures Printed by 3D Food Printer. *Jpn. J. Food Eng.* **2021**, *22*, 119–134. [CrossRef]
19. Liu, Z.; Dick, A.; Prakash, S.; Bhandari, B.; Zhang, M. Texture modification of 3D printed air-fried potato snack by varying its internal structure with the potential to reduce oil content. *Food Bioprocess Technol.* **2020**, *13*, 564–576. [CrossRef]
20. Pulatsu, E.; Su, J.; Kenderes, S.M.; Lin, J.; Vardhanabhuti, B.; Lin, M. Restructuring cookie dough with 3D printing: Relationships between the mechanical properties, baking conditions, and structural changes. *J. Food Eng.* **2022**, *319*, 110911. [CrossRef]
21. Chen, X.; Zhang, M.; Teng, X.; Mujumdar, A.S. Internal structure design for improved shape fidelity and crispness of 3D printed pumpkin-based snacks after freeze-drying. *Food Res. Int.* **2022**, *157*, 111220. [CrossRef]
22. Lille, M.; Nurmela, A.; Nordlund, E.; Metsä-Kortelainen, S.; Sozer, N. Applicability of protein and fiber-rich food materials in extrusion-based 3D printing. *J. Food Eng.* **2018**, *220*, 20–27. [CrossRef]

23. Dick, A.; Bhandari, B.; Dong, X.; Prakash, S. Feasibility study of hydrocolloid incorporated 3D printed pork as dysphagia food. *Food Hydrocoll.* **2020**, *107*, 105940. [CrossRef]

24. Theagarajan, R.; Nimbkar, S.; Moses, J.A.; Anandharamakrishnan, C. Effect of post-processing treatments on the quality of three-dimensional printed rice starch constructs. *J. Food Process Eng.* **2021**, *44*, e13772. [CrossRef]

25. Liu, Y.; Tang, T.; Duan, S.; Qin, Z.; Zhao, H.; Wang, M.; Li, C.; Zhang, Z.; Liu, A.; Han, G.; et al. Applicability of Rice Doughs as Promising Food Materials in Extrusion-Based 3D Printing. *Food Bioprocess Technol.* **2020**, *13*, 548–563. [CrossRef]

26. Thangalakshmi, S.; Arora, V.K.; Kaur, B.P.; Singh, R.; Malakar, S.; Rathi, S.; Tarafdar, A. Effect of Steaming as Postprocessing Method on Rice Flour and Jaggery 3D Printed Construct. *J. Food Qual.* **2022**, *2022*, 3531711. [CrossRef]

27. Semba, R.D.; Ramsing, R.; Rahman, N.; Kraemer, K.; Bloem, M.W. Legumes as a sustainable source of protein in human diets. *Glob. Food. Sec.* **2021**, *28*, 100520. [CrossRef]

28. Arab, E.; Helmy, I.; Bareh, G. Nutritional evaluation and functional properties of chickpea (*Cicer arietinum* L.) flour and the improvement of spaghetti produced from its. *J. Am. Sci.* **2010**, *6*, 1055–1072.

29. InTech. *Functional Food—Improve Health through Adequate Food*; InTech: London, UK, 2017. [CrossRef]

30. Dick, A.; Bhandari, B.; Prakash, S. Post-processing feasibility of composite-layer 3D printed beef. *Meat Sci.* **2019**, *153*, 9–18. [CrossRef]

31. Dong, X.; Huang, Y.; Pan, Y.; Wang, K.; Prakash, S.; Zhu, B. Investigation of sweet potato starch as structural enhancer for 3D printing of *Scomberomorus niphonius* surimi. *J. Texture Stud.* **2018**, *50*, 316–324. [CrossRef]

32. Bourne, M.C. Chapter 4-Principles of Objective Texture Measurement. In *Food Texture and Viscosity*; Bourne, M.C., Ed.; Academic Press: London, UK, 2002; pp. 107–188. ISBN 978-0-12-119062-0.

33. Barrett, A.H.; Cardello, A.V.; Mair, L.; Maguire, P.; Lesher, L.L.; Richardson, M.; Briggs, J.; Taub, I.A. Textural Optimization of Shelf-Stable Bread: Effects of Glycerol Content and Dough-Forming Technique. *Cereal Chem.* **2000**, *77*, 169–176. [CrossRef]

34. Berthaume, M.A. Food mechanical properties and dietary ecology. *Am. J. Phys. Anthropol.* **2016**, *159*, 79–104. [CrossRef]

35. Gibson, L.J.; Ashby, M.F. *Cellular Solids: Structure and Properties*, 2nd ed.; Cambridge University Press: Cambridge, UK, 1997.

36. Assad-Bustillos, M.; Tournier, C.; Feron, G.; Guessasma, S.; Reguerre, A.L.; Della Valle, G. Fragmentation of two soft cereal products during oral processing in the elderly: Impact of product properties and oral health status. *Food Hydrocoll.* **2019**, *91*, 153–165. [CrossRef]

37. Aguilera, J.M.; Stanley, D.W. *Microstructural Principles of Food Processing and Engineering*, 2nd ed.; Springer: New York, NY, USA, 1999.